THE DESIGN OF A LARGE BOOSTER RING FOR THE MEDIUM ENERGY ELECTRON-ION COLLIDER AT JLAB*

E. Nissen#, T. Satogata, Y. Zhang, Thomas Jefferson National Accelerator Facility, Newport News, VA 23606, USA

Abstract

In this paper, we present the current design of the large booster ring for the Medium energy Electron-Ion Collider at Jefferson Lab. The booster ring takes 3 GeV protons or ions of equivalent rigidity from a pre-booster ring, and accelerates them to 20 GeV for protons or equivalent energy for light to heavy ions before sending them to the ion collider ring. The present design calls for a figure-8 shape of the ring for superior preservation of ion polarization. The ring is made of warm magnets and shares a tunnel with the two collider rings. Acceleration is achieved by warm RF systems. The linear optics has been designed with the transition energy above the highest beam energy in the ring so crossing of transition energy will be avoided. Preliminary beam dynamics studies including chromaticity compensation are presented in this paper.

INTRODUCTION

The Medium energy Electron Ion Collider (MEIC) will be the first step towards a full energy Electron Ion Collider at Jefferson Lab. It will collide 3-11 GeV electrons with 20-100 GeV protons, or with other ions from deuterons up to lead, with energy up to 40 GeV per nucleon. These collisions will take place at two detectors in a ring-ring collider [1].

In the current MEIC baseline, a new ion complex must be constructed for accelerating and storing ion beams. Fig. 1 illustrates this multi-staged ion complex. In the rest of this paper, we will use a proton beam as an example for discussion; however, the design can also be applied to all ion species with energies adjusted accordingly, assuming the same magnetic rigidities of the rings. In this new ion complex, the protons are produced at the ion source, accelerated by an SRF linac into the pre-booster where they are accelerated to 3 GeV [2], then they are accelerated in the large booster to 20 GeV, before they are sent to the ion collider ring where they reach their final collision energy. This paper will focus on design of the large booster ring, which is similar in function to other booster rings [3]. All the ion booster and collider rings of the MEIC have a figure-8 shape for an exact cancellation of spin precession in the stored electrons and ions. This will enable experiments with high levels (>70%) of polarization.

In addition, a staged electron cooling scheme is used to achieve and preserve small transverse beam emittance and very short bunch length for increased luminosity. Low energy electron cooling occurs in the pre-booster, while high energy electron cooling occurs in the collider ring.

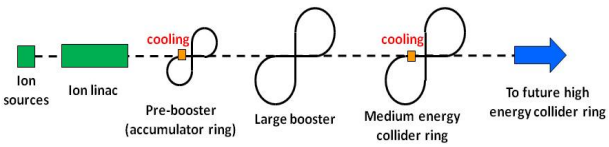

Figure 1: Outline of the MEIC Ion Complex.

LARGE BOOSTER DESIGN

Design Constraints

Presently, the large booster is in a vertical stack which includes the electron and ion collider rings, thus requiring footprints of the three rings to be nearly identical in order to be housed in a same tunnel. Since the two collider rings contain many critical components such as interaction regions (IR), their layouts should be determined first, then matched by the large booster ring. The large booster is designed with warm magnets which puts a limit on the available dipole field, as well as multipole pole tip fields of 1.7 T. To avoid particle loss from transition crossing, the transition energy should be above 20 GeV, namely, γ_{tr}>22.32.

Ring Design

Currently, the collider rings are designed with four identical 120° arc sections separated by two long straights (containing IRs) and two short straights (for Siberian snakes). In addition, the electron collider ring has one Universal Spin Rotator of nearly 50 m long on the end of each arc near a long straight. The large booster will be designed similarly to match the geometry of the collider rings. The layout of the large booster is shown in Fig. 2. A matching block is placed at each end of an arc to follow geometry of the spin rotators in the electron ring.

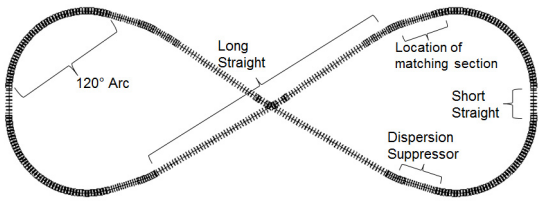

Figure 2: An outline of the large booster with the building blocks labelled.

Linear Optics Design

In the interests of simplicity, and preserving a high transition energy, the basic building block of the large

#nissen@jlab.org

booster is a FODO lattice. The arcs must hold a total of 240° of bending for each side, including matching sections. The arc FODO sections have been chosen such that there is sufficient space for the quadrupoles, dipoles, as well as sextupoles for chromaticity compensation. This required an optimization of the size of the bending dipoles used in the large booster. If they are too long then not enough FODO cells are used, and the transition γ becomes too low. If they are too short then it becomes difficult to match the geometry of the spin rotators. The Twiss functions of an arc FODO cell are shown in Fig. 3.

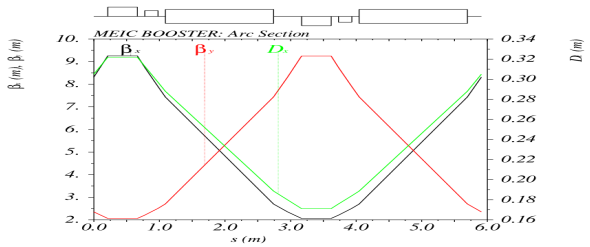

Figure 3: The Twiss functions of an arc FODO cell. The two small short rectangles indicate two sextupoles.

The dispersion at the ends of the arcs is suppressed using variation of quad strengths in the matching block. A diagram of the dispersion suppression section is shown in Fig. 4. Since the dipoles in the arc and in the matching block are not the same, the dispersion in this section is not symmetric.

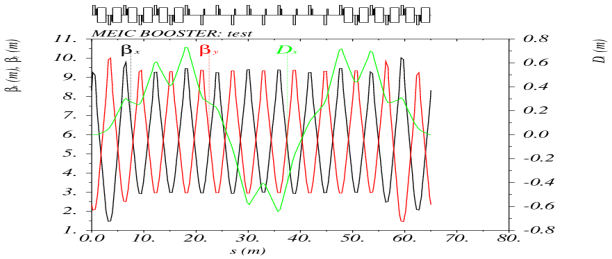

Figure 4: The Twiss functions of a dispersion suppression section.

The arcs are connected to each other with long straight sections, which contain a set of small bends to follow the geometry of the IRs in the collider rings. The optics is matched between the entrances and exits of the arcs. Using two sets of seven FODO cells in each section, any fractional betatron tune can be reached. A diagram of the optics for the long straight section is shown in Fig. 5. The smaller bends which are needed to follow the geometry of the IRs use a double bend achromat type of layout to avoid dispersion leakage in the rest of the section. As can be seen at the 245 meter mark in Fig 5, to allow the double bend achromat to work properly, the lattice is shortened to match the final bend spacing so that the cells needed to match into that section are not in an area that requires bending, between the 220 and 245 meter marks.

There are short straight sections on the ends of the ring between the two arcs, which is currently filled with a set of FODO cells with a unit matrix as a transfer map. This is a placeholder for future machine elements. The optics of the entire booster is shown in Fig. 6.

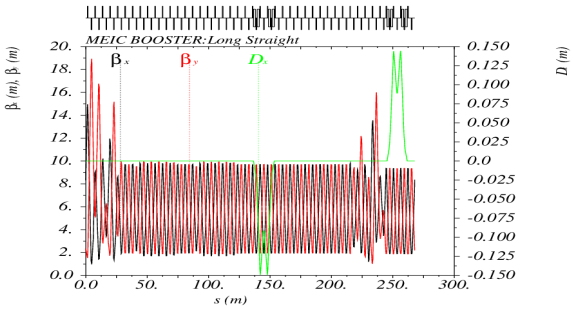

Figure 5: The optics of one of the long straight sections in the large booster.

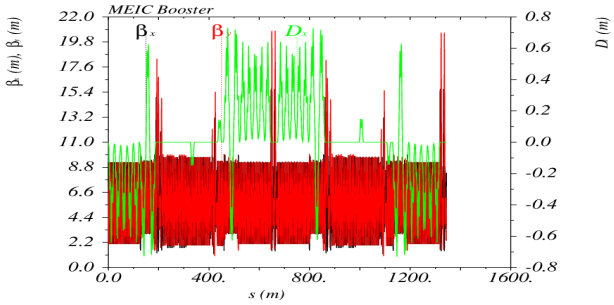

Figure 6: Linear optics of the large booster.

Both for simplification and for cost savings the number of types of magnets have been minimized in this design. Table 1 contains a complete list of the number and types of magnet elements in the large booster.

Table 1: Magnetic Elements in the Large Booster

Quantity	Unit	Value
Arc Dipole Number		204
Straight Dipole Number		16
Arc Dipole Length	m	1.65
Straight Dipole Length	m	1.65
Arc Dipole Field Strength	T	1.64
Straight Dipole Field Strength	T	0.769
Arc Dipole Bend Radius	m	42.49
Straight Dipole Bend Radius	m	90.65
Arc Dipole Bend Angle	Deg.	2.225
Straight Dipole Bend Angle	Deg.	1.043
Arc Quad number		192
Straight quad number		286
Arc/Straight Quad Length	m	0.45
Arc Quad Gradient	T/m	75.22
Straight Quad Gradient	T/m	75.59
Arc Sextupole number		256
Arc Sextupole Length	m	0.2
Arc sextupole k2	1/m²	20/-33

Longitudinal Design

A preliminary analysis of the acceleration system gives a baseline dipole magnet ramping rate of 1.5 T/s. Thus it takes 0.95 s (approximately 214,000 turns in the booster ring) to ramp the dipole field to the peak value of 1.65 T. We used two RF cavities in the design that were placed in the dispersion free region of the short straight section. Assuming that the beam is accelerated 45° off crest, then each cavity is 120 kV. The total RF power needed to accelerate a beam of 0.5 A current would be 60 kW. The synchrotron tunes, as well as other quantities of interest to the large booster are shown in Table 2.

Table 2: Linear Parameters for the Large Booster in the Medium Energy Electron Ion Collider

Quantity	Unit	Value
Proton kinetic energy	GeV	3 to 20
Ion rigidity at injection	Tm	12.76
Ion Rigidity at extraction	Tm	69.77
Ring circumference	m	1343.9
Figure-8 crossing angle	Deg.	60
Quarter arc length	m	189.1
Length of long straight	m	267.8
Length of short straight	m	25.9
Lattice base cell		FODO
Arc cell length	m	5.91
Straight section cell length	m	6.1
Phase Advance per cell in arc	Deg.	85.7
Phase advance per cell in straight	Deg.	90
FODO cells in arcs		32
FODO cells in straights		43
Dispersion Suppression Method		Phase Advance
Max. horiz. beta function	m	15.0
Max. vert. beta function	m	19.0
Maximum horiz. Dispersion	m	0.73
Horizontal betatron tunes		53.41
Vertical betatron tune		52.58
Synchrotron tune injection	$x10^{-2}$	.149
Synchrotron tune extraction	$x10^{-4}$	.536
natural horiz. chromaticity		-67.42
natural vertical chromaticity		-67.36
Transition Energy factor γ_{tr}		25.028
Horizontal/vertical normalized emittance	mm·mrad	4
Max. horiz. rms beam size	mm	7.7
Max. vert. rms beam size	mm	8.8
Laslett Tune shift injection		-.1
Laslett Tune shift extraction		-.0035

The Laslett tune shift was calculated at both injection and extraction assuming an bunching factor of 0.5, and current design values for other quantities. The values shown do not present any major problems.

BEAM DYNAMICS

The large booster's linear dynamics are straightforward as shown in the previous section; however nonlinear dynamics also have to be taken into account. The chromaticities are compensated by using two families of sextupoles in the arcs since the arcs have the largest dispersion.

While a full working point analysis has not been performed, a manual scan of fractional tunes has yielded a set of magnet settings that maintain stable orbits out to ~9 or 10 standard deviations. A method of visualizing this is done by placing particles with zero angle in phase space on the axis at set distances equal different multiples of the standard deviation. An example of this is shown for the horizontal phase space motion in Fig. 7. Orbits can remain stable under these tunes out to 10 standard deviations.

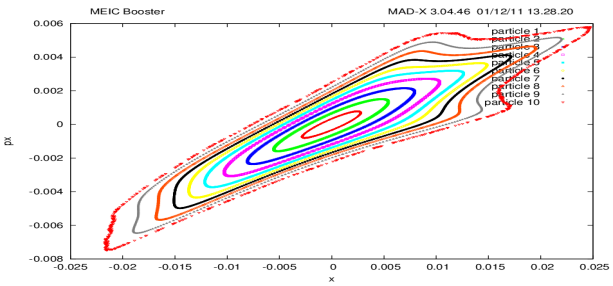

Figure 7: Ten orbits started at 1 through 10 standard deviations radially in horizontal phase space. They are advanced through 1000 turns to examine orbit stability.

CONCLUSIONS

The linear design of the MEIC large booster ring has been completed. The overall geometry of the ring conforms to the tunnel shared by the electron and ion collider rings. The FODO cells in the long straight sections provide sufficient variability in betatron tune that the ring can hit any fractional tune desired. Some initial work has been done to compensate for the effects of chromaticity. Preliminary work has also been performed to calculate dynamic quantities such as Laslett tune shift, and the RF acceleration requirements of the machine.

ACKNOWLEDGEMENTS

The authors would like to thank Vasiliy Morozov for providing design information of the MEIC collider rings and for helpful discussion.

REFERENCES

[1] Y. Derbenev et. al., "MEIC Design Status," TUPPR082, These Proceedings.

[2] B Erdelyi et. al., "An Accumulator/Prebooster for the Medium-Energy Electron Ion Collider at Jlab," PAC '11, New York, March 2011,WEP206.

[3] E. Courant and Z. Parsa, "The Booster Lattice," Booster Technical Note, Brookhaven National Laboratory, (1986)